Bounded Nonlinear Stabilizing Speed Regulators for VSI-Fed Induction Motors in Field-Oriented Operation

George C. Konstantopoulos, *Member, IEEE*, Antonio T. Alexandridis, *Member, IEEE*, and Epaminondas D. Mitronikas, *Member, IEEE*

***Abstract*— A new nonlinear controller design is developed for speed regulation of voltage source inverter (VSI)-driven induction motors. The proposed controller directly provides the duty-ratio input of the VSI in the permitted range to ensure linear modulation, is fully independent from the system parameters and suitably regulates the motor speed and the stator flux to the desired values. Considering the complete nonlinear model of the converter-motor system and applying advanced nonlinear methods, boundedness of the full system states is proven. Furthermore, exploiting the Hamiltonian-passive structure of the system, state convergence to the equilibrium is shown using LaSalle's Invariance Principle. Though the controller design is developed in the frame of the field-oriented control methodology, stability holds true even without accurate field orientation guaranteeing an effective performance in cases where parameter variations occur. Extensive simulation results on an industrial size system are conducted to evaluate the proposed controller performance, under rapid changes of the reference speed or load torque as well as system parameter variations. In addition, a lab size induction motor system is experimentally tested. In all cases, the system response shows fast convergence to the equilibriums after limited transients, thus verifying the theoretical results.**

***Index Terms*— Induction motor control, nonlinear control systems, stability.**

I. Introduction

TRADITIONALLY induction motor is the most widely used electrical machine in simple industrial applications, because of its low cost and increased reliability. In the last decades, the development of high power, cheap, and reliable power electronic converters provides a great opportunity of using medium or large induction machines in many advanced industrial drive applications [1]. Hence other motor types, such as dc motors and so forth, are gradually replaced by the squirrel cage induction machine usually driven by a voltage source inverter (VSI) power electronic device.

The effective implementation of high demanding ac drives and control is not an easy task, caused by some inherent difficulties of the system dynamics. The significant difference between the mechanical and the electrical system time constant but mainly the nonlinear dynamic performance of an induction motor that is additionally increased by the extra nonlinearities of the VSI dynamics and the switching performance, constitute the main obstacles in control designs. In addition, as pulsewidth modulation (PWM) is the standard technique through which the control law is applied on the VSI, the controlled input actually is the duty-ratio input of the converter. Duty-ratio input is, however, not yet an "affine input" of the system while it has to be strictly bounded in a specific range. As all these should be considered, they create additional difficulties on the control design and especially on proving stability.

Early control designs concerned with ac drives are based on linear systems theory [2] and use precompensating terms to transform part of the nonlinear system to a linear form. Control schemes that include feedback linearization methods [3], are effective in neglecting all the nonlinearities but are sensitive to model uncertainties. Sliding mode techniques [4] seem to be more effective but their main drawback is that they cannot guarantee closed-loop system stability under unknown load torque disturbances.

In nonlinear control designs, Hamiltonian analysis and passivity-based controllers [5]–[7] seem to be adequately efficient. Unfortunately, most of these methods are also highly dependent from the system parameters. Backstepping [8] and adaptive backstepping [9] control schemes are widely used to compensate unknown model parameters and variations, which, however, cannot be fully independent from essential system parameters.

Nowadays, the most common control methodology relies on vector control (or field-oriented technique) [10] that simplifies the electromagnetic torque expression as in a separately excited dc motor. The vector control method is, however, a complex and demanding technique, while it is dependent on the system parameters, some inaccessible states and the external unknown load torque disturbances. In particular, vector control analysis is conducted on the synchronously rotating $d-q$ reference frame because all sinusoidal quantities are transformed into dc quantities in steady-state. This makes possible a more efficient control design that can regulate the transformed system states to the desired constant equilibrium. In this frame, the indirect rotor field oriented control (IR-FOC) methodology is widely and successfully applied to provide high performance operation with induction motor drives [1], [2]. This scheme provides rotor speed regulation and maintains constant flux with the main advantage that it does not require rotor flux sensors or an estimate of flux angle [1], [2]. A main drawback, however, is that it requires the knowledge of the rotor time constant, a parameter which can vary largely during drive's operation. This mismatch causes loss of field orientation leading to significant

Manuscript received September 6, 2012; accepted June 8, 2013. Manuscript received in final form June 22, 2013. Date of publication July 24, 2013; date of current version April 17, 2014. This work was supported by the Greek State Scholarships Foundation. Recommended by Associate Editor F. Vasca.

G. C. Konstantopoulos was with the Department of Electrical and Computer Engineering, University of Patras, Rion 26500, Greece. He is now with the Department of Automatic Control and Systems Engineering, University of Sheffield, Sheffield S1 3JD, U.K. (e-mail: g.konstantopoulos@sheffield.ac.uk).

A. T. Alexandridis and E. D. Mitronikas are with the Department of Electrical and Computer Engineering, University of Patras, Rion 26500, Greece (e-mail: a.t.alexandridis@ece.upatras.gr; e.mitronikas@ece.upatras.gr).

Digital Object Identifier 10.1109/TCST.2013.2271256

performance and stability problems [1]. At the controller design implementation level, two basic schemes are used: the so-called current hysteresis band (HB) control scheme or the cascaded linear or nonlinear proportional-integral (PI), RST, and so on controller scheme with the slow outer-loops to provide the reference current values for the fast inner-current loops [1]. The latter scheme is clearly better as the rating of the system becomes larger, but to be effective, its design requires complete decoupling compensation of the system nonlinearities, thus increasing the dependence from the system parameters. Finally, external limiters should be used such as the controller output to provide the duty-ratio signal input of the VSI device in the permitted range.

In this brief, a new simple nonlinear controller design is developed suitable for speed regulation of a VSI-driven induction motor. For the analysis, the complete nonlinear model is used consisting of the motor model and the average nonlinear model of the inverter [5], [7]. The proposed controller directly provides the duty-ratio input of the VSI exactly in the permitted range that ensures linear modulation [1], is fully independent from the system parameters and additionally regulates the rotor speed and maintains constant flux through the d-axis stator current at the desired values in the frame or independently from the IR-FOC methodology. Closed-loop stability of the complete system is proven in detail using advanced nonlinear methods for obtaining state boundedness, whereas the general concept described in [11] and [12] is applied to guarantee convergence to the equilibrium. As shown in the brief, stability is proven even far from field orientation, guaranteeing an effective performance in any parameter and time constant variations. Simulation results verify the proposed simple controller performance under several speed reference changes and load torque disturbances for a 22.4-kW induction motor by considering constant or varying rotor time constants. Experimental results on a lab size 1.5-kW induction motor are also presented to further confirm the theoretical analysis.

In Section II, the nonlinear dynamic model of an induction motor is presented and a quick background of the conventional IR-FOC technique is underlined. In Section III, the complete dynamic model of an induction motor with a three-phase VSI device fed by a dc-link is developed. In Section IV, the proposed simple nonlinear speed regulator is extensively analyzed by investigating and proving its stability properties. In Section V, the controller performance is tested through extended simulation results, whereas in Section VI experimental results are provided. Finally, in Section VII some conclusions are summarized.

II. Induction Motor Modeling and Conventional Vector Control Analysis

Fig. 1 shows the system under consideration, consisting of an induction motor connected to the three-phase power supply through a three-phase diode rectifier, a dc-link and a VSI. C is the dc-side capacitor while L and R_L represent the small inductance and resistance that appears in a dc-link. Using the synchronously rotating $d-q$ reference frame, well known as Park's transformation [1] in which all the sinusoidal quantities

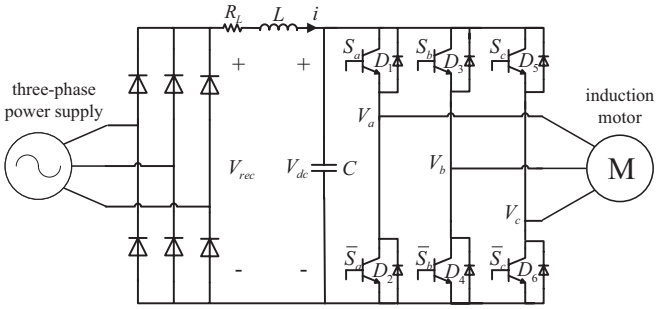

Fig. 1. Schematic diagram of the system under consideration.

are transformed into dc quantities in steady-state, the dynamic equations of the squirrel-cage induction motor are given as follows:

$$\begin{aligned} V_{ds} &= R_s i_{ds} + \dot{\lambda}_{ds} - \omega_s \lambda_{qs} \\ V_{qs} &= R_s i_{qs} + \dot{\lambda}_{qs} + \omega_s \lambda_{ds} \\ 0 &= R_r i_{dr} + \dot{\lambda}_{dr} - (\omega_s - p\omega_r)\,\lambda_{qr} \\ 0 &= R_r i_{qr} + \dot{\lambda}_{qr} + (\omega_s - p\omega_r)\,\lambda_{dr} \end{aligned} \tag{1}$$

where i_{ds}, i_{qs}, and i_{dr}, i_{qr} are the d and q axis components of the stator and rotor currents, respectively, λ_{ds}, λ_{qs} and λ_{dr}, λ_{qr} are the d and q axis components of the stator and rotor fluxes, respectively, V_{ds} and V_{qs} are the d and q axis components of the stator voltage. Parameters R_s and R_r are the stator and rotor resistances, respectively, ω_s is the synchronous speed (reference frame), ω_r is the rotor speed, and p is the number of pole pairs. The fluxes are combined with the currents according to the following expressions:

$$\begin{aligned} \lambda_{ds} &= L_{ls} i_{ds} + L_m\,(i_{ds} + i_{dr}) = L_s i_{ds} + L_m i_{dr} \\ \lambda_{qs} &= L_{ls} i_{qs} + L_m\,(i_{qs} + i_{qr}) = L_s i_{qs} + L_m i_{qr} \\ \lambda_{dr} &= L_{lr} i_{dr} + L_m\,(i_{ds} + i_{dr}) = L_r i_{dr} + L_m i_{ds} \\ \lambda_{qr} &= L_{lr} i_{qr} + L_m\,(i_{qs} + i_{qr}) = L_r i_{qr} + L_m i_{qs} \end{aligned} \tag{2}$$

where $L_s = L_{ls} + L_m$ and $L_r = L_{lr} + L_m$ are the stator and rotor inductances, respectively, and L_m is the mutual inductance.

In addition, the torque equation that describes the relationship between the motor torque and the rotor speed is as follows:

$$T_e = T_L + J_m \dot{\omega}_r + b\omega_r \tag{3}$$

where J_m is the total motor and load inertia, b is the friction coefficient, and T_L is the load torque, whereas the electromagnetic torque of the motor is given as follows:

$$T_e = \frac{3}{2} p \frac{L_m}{L_r} \left(\lambda_{dr} i_{qs} - \lambda_{qr} i_{ds}\right). \tag{4}$$

IR-FOC technique relies on operating the induction motor as a separately excited dc motor. In most applications, the indirect field orientation is applied where the total rotor flux λ_r is aligned on the synchronous rotating d-axis

$$\lambda_r = \lambda_{dr}, \quad \lambda_{qr} = 0. \tag{5}$$

This operation decouples the rotor flux dynamic equations leading to simplified control design. Applying (5) to the nonlinear dynamic model (1) and assuming steady-state operation,

we can determine the desired slip frequency from the 4th equation of (1) as follows:

$$\omega_s - p\omega_r \equiv \omega_{sl} = \frac{L_m}{\tau_r \lambda_r} i_{qs} \tag{6}$$

where $\tau_r = L_r/R_r$ is the rotor time constant. Because the rotor flux cannot be measured, the amplitude of the flux is usually estimated from the 3rd equation of system (1) as follows:

$$\tau_r \dot{\hat{\lambda}}_r + \hat{\lambda}_r = L_m i_{ds} \tag{7}$$

where $\hat{\lambda}_r$ is the estimation of the total rotor flux [13]. Assuming the induction motor is operated below the rated speed, the rotor flux should be maintained constant and therefore the reference signals are the desired motor speed ω_r^{ref} and the rotor flux $\bar{\lambda}_r$. Assuming steady-state operation, $\hat{\lambda}_r = \bar{\lambda}_r$, we can define from (7) the constant d-axis current $\bar{i}_{ds}$ as follows:

$$\bar{\lambda}_r = L_m \bar{i}_{ds}. \tag{8}$$

Thus, conventional IR-FOC techniques [1] require the use of three PI controllers wherein: 1) a PI controller is used at the stator input voltage V_{ds} to maintain the d-axis current at $\bar{i}_{ds}$ and 2) two cascaded PI controllers are used to control the rotor speed through the q-axis current of the stator. In particular, the first inner-loop PI controller, used at the stator voltage V_{qs}, regulates current i_{qs} at its reference $\bar{i}_{qs}$, whereas the second outer-loop PI controller provides the $\bar{i}_{qs}$ value by comparing the measured motor speed ω_r with the desired reference ω_r^{ref}. Inner-loop PI controller design is based on the linear systems theory and therefore decoupling terms are usually added to provide stability [13]. This decoupling is also needed to ensure precise field orientation during transients, i.e., to ensure the rotor flux to be kept constant at all times. Although the use of compensating terms results in a linear system that permits a direct gain selection for the inner-loop PI controllers, the dependence of the control design from the system parameters increases, thus increasing the controller sensitivity in parameter uncertainties. Furthermore, because the final control is implemented on the duty-ratio signal input of the VSI, saturators that can limit the controller outputs in the permitted range are needed.

Alternatively, HB controllers can be used to produce the appropriate pulses for the VSI. However, neither analytical modeling of the HB controller nor stability analysis are guaranteed in this case [1].

To prove global asymptotic stability of the induction motor using IR-FOC, several researchers use the reduced-order current-fed model of the motor, i.e., a third-order system with states the rotor fluxes and the motor speed and control inputs the stator currents [14]–[17]. In these cases, the inverter and dc-link dynamics are completely ignored. Some researchers, working on the fifth-order model of the induction motor as provided from (1)–(3), can prove asymptotic stability in IR-FOC operation [13], [18]–[24] only under the use of parameter or load torque estimators or adaptation mechanisms, with the inverter assumed to operate as an ideal current source.

For a rigorous stability analysis, it becomes clear that the complete model of the three-phase VSI device and the induction motor is required in combination or without the IR-FOC technique, because the nonlinear dynamics of the VSI should be considered. According to the authors' knowledge, stability analysis using the IR-FOC technique on the complete VSI-fed induction motor model is not yet exploited. Thus, in this brief, a nonlinear controller is proposed that besides its other enhanced characteristics, can guarantee stability of the whole system in field- or near field-oriented operation.

III. Complete System Model of a VSI-Fed Induction Motor

Assuming as state variables of the induction motor the stator currents i_{ds}, i_{qs}, the rotor fluxes λ_{dr}, λ_{qr}, and the motor speed ω_r and adding to these the state variables of the dc-link, i.e., the capacitor voltage V_{dc} and the dc-link inductance current i, the dynamic model of the complete system (Fig. 1) is obtained. Because the original three-phase model of the system contains discontinuous input terms, and because of the switching functions caused by the PWM operation, the averaging analysis for the VSI device [5], [7] is adopted to obtain a continuous model suitable for control purposes. Furthermore, using the synchronously rotating $d-q$ reference frame, both the ac and dc sides of the system are represented by nonsinusoidal states and parameters. Thus, finally the complete system takes the following nonlinear matrix form:

$$M\dot{x} = \left(J\left(x, m_{ds}, m_{qs}\right) - R\right)x + G\epsilon \tag{9}$$

with (10) shown at the top of the next page, where the state vector is $x = [\, i_{ds}\ i_{qs}\ \lambda_{dr}\ \lambda_{qr}\ \omega_r\ i\ V_{dc}\,]^T$, the external uncontrolled input vector is $\epsilon = [-(2/3)T_L \quad (2/3)V_{\text{rec}}]^T$, with V_{rec} being the dc output voltage of the three-phase diode rectifier and parameter σ is given as $\sigma = L_s - L_m^2/L_r$.

Variables m_{ds} and m_{qs} are defined as $m_{ds} = V_{ds}/(2V_{dc})$ and $m_{qs} = V_{qs}/(2V_{dc})$ and represent the d and q-axis controlled input components [25], namely the switching duty-ratio components for which it holds true that [1]

$$m_a = \sqrt{m_{ds}^2 + m_{qs}^2} \tag{11}$$

with m_a being the switching duty ratio of phase$-a$ of the induction motor voltage in a period under PWM regulation (modulation index) and $\Delta\phi$ is the initial phase of the induction motor phase-a voltage

$$\Delta\phi = \arctan\left(\frac{m_{qs}}{m_{ds}}\right). \tag{12}$$

Furthermore, in most motor control applications, it is preferred that the inverter operates in the "linear modulation" area [25] to avoid the existence of higher harmonics. This means that

$$m_a \leq 1.$$

Therefore, considering (11), it should be [1]

$$m_{ds}^2 + m_{qs}^2 \leq 1. \tag{13}$$

Because the system is connected to a symmetrical three-phase power supply, the output voltage of the diode rectifier V_{rec} is assumed to be constant and because T_L is the disturbance torque input, the only controlled inputs are the

$$M = \operatorname{diag}\left\{\sigma, \sigma, \frac{1}{L_r}, \frac{1}{L_r}, \frac{2J_m}{3}, \frac{2L}{3}, \frac{2C}{3}\right\}$$

$$J = \begin{bmatrix} 0 & \sigma\omega_s & 0 & 0 & \frac{L_m}{L_r}p\lambda_{qr} & 0 & 2m_{ds} \\ -\sigma\omega_s & 0 & 0 & 0 & -\frac{L_m}{L_r}p\lambda_{dr} & 0 & 2m_{qs} \\ 0 & 0 & 0 & \frac{\omega_s - p\omega_r}{L_r} & 0 & 0 & 0 \\ 0 & 0 & -\frac{\omega_s - p\omega_r}{L_r} & 0 & 0 & 0 & 0 \\ -\frac{L_m}{L_r}p\lambda_{qr} & \frac{L_m}{L_r}p\lambda_{dr} & 0 & 0 & 0 & 0 & 0 \\ 0 & 0 & 0 & 0 & 0 & 0 & -\frac{2}{3} \\ -2m_{ds} & -2m_{qs} & 0 & 0 & 0 & \frac{2}{3} & 0 \end{bmatrix}$$

$$G = \begin{bmatrix} 0 & 0 & 0 & 0 & 1 & 0 & 0 \\ 0 & 0 & 0 & 0 & 0 & 1 & 0 \end{bmatrix}^T$$

$$R = \begin{bmatrix} \frac{R_r L_m^2}{L_r^2} + R_s & 0 & -\frac{R_r L_m}{L_r^2} & 0 & 0 & 0 & 0 \\ 0 & \frac{R_r L_m^2}{L_r^2} + R_s & 0 & -\frac{R_r L_m}{L_r^2} & 0 & 0 & 0 \\ -\frac{R_r L_m}{L_r^2} & 0 & \frac{R_r}{L_r^2} & 0 & 0 & 0 & 0 \\ 0 & -\frac{R_r L_m}{L_r^2} & 0 & \frac{R_r}{L_r^2} & 0 & 0 & 0 \\ 0 & 0 & 0 & 0 & \frac{2}{3}b & 0 & 0 \\ 0 & 0 & 0 & 0 & 0 & \frac{2}{3}R_L & 0 \\ 0 & 0 & 0 & 0 & 0 & 0 & 0 \end{bmatrix} \tag{10}$$

duty ratios m_{ds} and m_{qs} that appear in nonlinear terms. Furthermore, because the synchronous speed ω_s is produced from the inverter, it can also be specified by the control operator [1] accordingly to the desired slip frequency ω_{sl}

$$\omega_s = p\omega_r + \omega_{sl}. \tag{14}$$

In (9), matrix M is positive definite, J is skew symmetric, and R is semipositive definite. Using the storage function $H(x) = (1/2)x^T Mx$, it can be easily proven that system (9) is equivalent to the generalized Hamiltonian-passive form as determined in [11] and [26].

IV. Proposed Nonlinear Control Design and Analysis

A. Proposed Nonlinear Controller and Closed-Loop System Model

Because of the nonlinearities of the complete model of the inverter-fed induction motor and because a small parameter variation may disorient the rotor flux, in this brief, a simple nonlinear controller is proposed that directly provides the duty-ratio input in the permitted range of operation, as it is determined by (13). The proposed scheme guarantees that the rotor flux λ_r can be oriented on the synchronous rotating d-axis at steady-state operation if the rotor time constant is precisely known. As it is shown, however, by the stability analysis used in this brief, which is conducted on the full system model, it is certified that in parameter mismatch, the proposed controller still guarantees stability and convergence to the desired equilibrium even when the rotor flux is not correctly oriented.

The proposed nonlinear duty-ratio controller is of the following simple form:

$$m_{ds} = z_1 \tag{15}$$

$$m_{qs} = z_2 \tag{16}$$

where

$$\dot{z} = A_{\text{contr}}(z, \omega_r, i_{ds})\, z \tag{17}$$

with

$$A_{\text{contr}} = \begin{bmatrix} 0 & 0 & -k_1\left(i_{ds} - i_{ds}^{\text{ref}}\right) \\ 0 & 0 & -k_2\left(\omega_r - \omega_r^{\text{ref}}\right) \\ k_1\left(i_{ds} - i_{ds}^{\text{ref}}\right) & k_2\left(\omega_r - \omega_r^{\text{ref}}\right) & -c\left(z_1^2 + z_2^2 + z_3^2 - r^2\right) \end{bmatrix}.$$

States $z = \begin{bmatrix} z_1 & z_2 & z_3 \end{bmatrix}^T$ represent the controller dynamics, k_1, k_2 are the two nonzero constant gains and c is the positive constant. Parameter r is defined as follows:

$$r^2 = z_1^2(0) + z_2^2(0) + z_3^2(0)\ \forall z_1(0), z_2(0), z_3(0) \tag{18}$$

and is arbitrarily selected whereas ω_r and ω_r^{ref} are the measured and desired motor speed, respectively, whereas i_{ds} and i_{ds}^{ref} are the measured and desired d-axis stator current, respectively.

For $\omega_r - \omega_r^{\text{ref}}$ and $i_{ds} - i_{ds}^{\text{ref}}$ bounded, the structure of the proposed controller (17) implies that the control law acts as an attractive limit cycle for the controller states z_1, z_2, and z_3 on the surface of a sphere C_r with center the origin and radius equal to r

$$C_r = \left\{z_1, z_2, z_3 : z_1^2 + z_2^2 + z_3^2 = r^2\right\}.$$

As it is obvious, by introducing the term $-c\left(z_1^2 + z_2^2 + z_3^2 - r^2\right)$ in (17) with r given by (18),

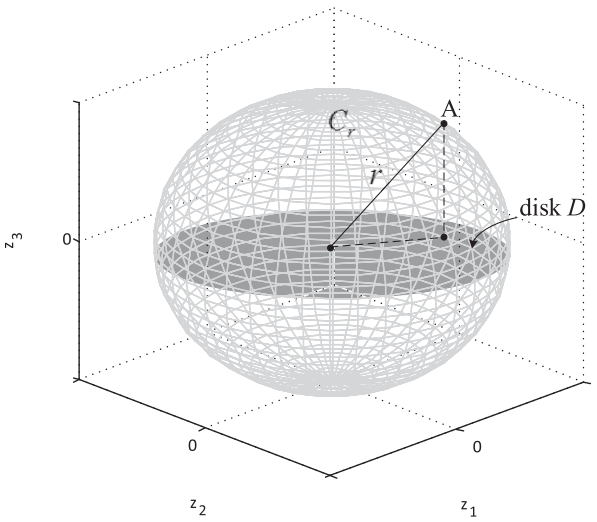

Fig. 2. Sphere C_r in $z_1 - z_2 - z_3$ space and disk D on $z_1 - z_2$ plane.

the controller states start and remain all time thereafter on sphere C_r. This means that the z_1, z_2, and z_3 trajectories rove over until they reach an equilibrium z_1^*, z_2^*, and z_3^* as ω_r and i_{ds} approach their reference values, whereas the robustness of z_1, z_2, and z_3 crucially increases in the sense that, if for any reason z_1^*, z_2^*, and z_3^* are disturbed, they cannot leave C_r.

Now, from the aforementioned controller analysis, it is immediately concluded that defining $r = 1$ then

$$(z_1(t))^2 + (z_2(t))^2 = 1 - (z_3(t))^2$$

with z_3 limited from C_r to be: $0 \leq (z_3(t))^2 \leq 1$. This means that $z_1(t)$ and $z_2(t)$ lie in a disk D with radius $r = 1$ (Fig. 2).

Considering (11) and (15), (16), the duty-ratio input becomes

$$m_a = \sqrt{(z_1(t))^2 + (z_2(t))^2} = \sqrt{1 - (z_3(t))^2}. \quad (19)$$

Hence, it is guaranteed that always $0 \leq m_a \leq 1$, i.e., the technical limits of the duty-ratio input are fulfilled. Thus, the proposed controller may provide a bounded control law exactly in the range permitted for linear modulation of the VSI device. The attractiveness of the controller solution guarantees robustness and controller response on the sphere C_r.

To hold all these controller properties true, it is essential to prove that i_{ds} and ω_r are bounded while as $i_{ds} \to i_{ds}^{\text{ref}}$ and $\omega_r \to \omega_r^{\text{ref}}$, the resulting z_1^* and z_2^* coincide with a stable solution of the entire system at the desired equilibrium. This is a cumbersome task and the proof is presented in the following sections.

Adopting rotor field orientation and assuming at steady-state that the rotor flux is aligned with the d-axis, then from (6) and (8) we arrive at the following expression for the slip frequency:

$$\omega_{sl} = \frac{1}{\tau_r i_{ds}^{\text{ref}}} i_{qs}. \quad (20)$$

Therefore, the synchronous speed is calculated, for a strictly nonzero value of i_{ds}^{ref}, as follows:

$$\omega_s = p\omega_r + \frac{1}{\tau_r i_{ds}^{\text{ref}}} i_{qs}. \quad (21)$$

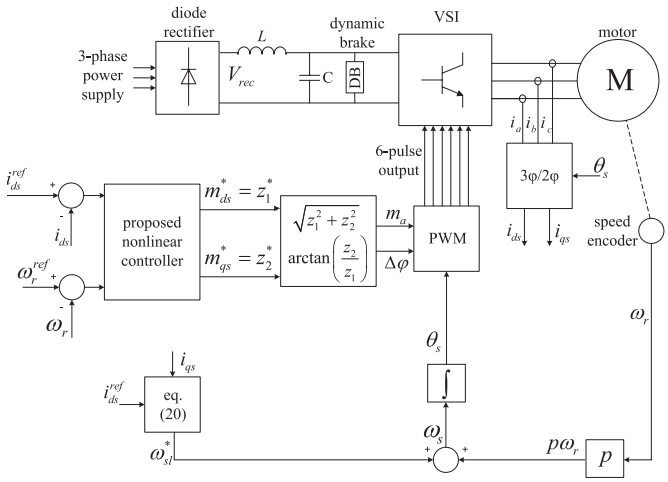

Fig. 3. Proposed nonlinear controller.

By considering $i_{ds}^{\text{ref}} = \bar{i}_{ds}$ with known τ_r, then field orientation is achieved with nominal flux in steady-state. In (20) and (21) the reference value of the d-axis stator current i_{ds}^{ref} is used rather than the measured variable i_{ds}, thus further simplifying the controller implementation. Furthermore, as it will be shown in the following section, the stability proof of the closed-loop system confronts the denominator $\tau_r i_{ds}^{\text{ref}}$ as an arbitrary constant by considering in general $\lambda_{qr} \neq 0$. This provides the flexibility to choose arbitrarily the denominator in (21), which means that the rotor time constant τ_r may not be exactly known, resulting in an incorrect rotor field orientation. Hence, without affecting stability, the proposed controller is designed to work in IR-FOC mode or independently from it (certainly within the motor capabilities), thus providing a clear superiority with respect to the existing techniques.

Introducing the proposed controller (15)–(17) and considering (21) in (9), the closed-loop system is given by the following 10th-order state-space representation:

$$\tilde{M}\dot{\tilde{x}} = \left(\tilde{J}(\tilde{x}) - \tilde{R}\right)\tilde{x} + \tilde{G}\epsilon \quad (22)$$

where the system matrices are

$$\tilde{M} = \begin{bmatrix} M & 0_{7\times 3} \\ 0_{3\times 7} & I_3 \end{bmatrix}$$
$$\tilde{G} = \begin{bmatrix} G^T & 0_{2\times 3} \end{bmatrix}^T$$
$$\tilde{R} = \begin{bmatrix} R & 0_{7\times 3} \\ 0_{3\times 7} & R_c \end{bmatrix}$$

with

$$R_c = \begin{bmatrix} 0_{2\times 2} & 0_{2\times 1} \\ 0_{1\times 2} & -c\left(z_1^2 + z_2^2 + z_3^2 - r^2\right) \end{bmatrix}$$

and $\tilde{J}$ as given in the Appendix. The closed-loop state vector is $\tilde{x} = [x^T \; z^T]^T = [i_{ds} \; i_{qs} \; \lambda_{dr} \; \lambda_{qr} \; \omega_r \; i \; V_{dc} \; z_1 \; z_2 \; z_3]^T$.

We can easily see that matrix $\tilde{M}$ remains symmetric and positive definite, $\tilde{J}$ is still skew-symmetric and $\tilde{R}$ matrix is symmetric. In addition, the system dynamics remain in its full form without any simplification caused by the field-oriented demand. The schematic diagram of the proposed nonlinear controller applied on the complete system is shown in Fig. 3.

B. Closed-Loop System Stability Analysis

Stability analysis and convergence to equilibrium that follows are directly linked with the Hamiltonian-passive structure of the closed-loop system [11]. This structure permits us to use the Hamiltonian function as Lyapunov storage function with obvious damping characteristics and to exploit some other system and controller structural characteristics for proving state boundedness in a region where a unique equilibrium exists. Finally, convergence to equilibrium is proven by suitably modifying and applying some recent results developed for these types of systems [11], [12]. Now, to proceed with the analysis, the following Proposition is first proven so that it ensures boundedness of the closed-loop system solution.

Proposition 1: Closed-loop system as given by (22) for some constant external input vector ϵ and controller initial conditions satisfying (18) with $r = 1$, is stable providing a bounded solution $\tilde{x}(t)$ in a region where a unique equilibrium exists.

Proof: To begin with the proof, we consider the closed-loop system (22) in the following form:

$$\dot{\tilde{x}} = A(\tilde{x})\,\tilde{x} + B\epsilon \tag{23}$$

where obviously $A(\tilde{x}) = \tilde{M}^{-1}\left(\tilde{J}(\tilde{x}) - \tilde{R}\right)$ and $B = \tilde{M}^{-1}\tilde{G}$. In (23), matrix $A(\tilde{x})$ can be written in the diagonal block form

$$A(\tilde{x}) = \begin{bmatrix} A_{\text{plant}}(x, z) & 0_{7\times 3} \\ 0_{3\times 7} & A_{\text{contr}}(z, \omega_r, i_{ds}) \end{bmatrix} \tag{24}$$

where $A_{\text{plant}}(x, z) = M^{-1}(J(x, z) - R)$ and $A_{\text{contr}}(z, \omega_r, i_{ds})$ is given directly from the controller dynamics (17) and

$$B = \begin{bmatrix} B_{\text{plant}}^T & B_{\text{contr}}^T \end{bmatrix}^T \tag{25}$$

with $B_{\text{plant}} = M^{-1}G$ and $B_{\text{contr}} = 0_{3\times 2}$.

Now, let us consider the nonlinear system (22) or (23) without the external input vector ϵ

$$\dot{\tilde{x}} = A(\tilde{x})\,\tilde{x}. \tag{26}$$

For system (26), we can consider the following storage function:

$$V = \frac{1}{2}\tilde{x}^T\tilde{M}\tilde{x} = \frac{1}{2}x^T M x + \frac{1}{2}z^T z. \tag{27}$$

Then, the time derivative of V is

$$\begin{aligned}\dot{V} &= x^T M M^{-1}(J(x, z) - R)\,x - c\left(z_1^2 + z_2^2 + z_3^2 - r^2\right)z_3^2 \\ &= -x^T R x - c\left(z_1^2 + z_2^2 + z_3^2 - r^2\right)z_3^2. \end{aligned} \tag{28}$$

Because matrix R is semipositive definite and considering (18), the second term $-c\left(z_1^2 + z_2^2 + z_3^2 - r^2\right)z_3^2$ is zero by definition and therefore (28) implies that $\dot{V} \leq 0$. This directly concludes that the unforced closed-loop system (26) is Lyapunov stable, i.e., all its states are bounded.

Furthermore, because (26) represents an autonomous system and the storage function $V(\tilde{x})$ is radially unbounded with nonpositive derivative over the whole state space, then in accordance to Global Invariant Set Theorem 3.5 described in [27], all solutions uniformly globally asymptotically converge to the largest invariant set N in E. Set E is defined as the set where $\dot{V} = 0$, i.e., as concluded from (28) with the given by (10) $R \geq 0$, set E consists of the union of $[\,i_{ds}\ i_{qs}\ \lambda_{dr}\ \lambda_{qr}\ \omega_r\ i\,]^T = 0$ and z constrained on the limit cycle described by sphere C_r and as from the sixth dynamic equation referred to state i, it is obvious that for $[\,i_{ds}\ i_{qs}\ \lambda_{dr}\ \lambda_{qr}\ \omega_r\ i\,]^T = 0$ also state V_{dc} can only satisfy the trivial solution. Therefore, invariant set N simply consists of the union of $x = 0$ and z constrained on the limit cycle described by sphere C_r.

The block diagonal structure of $A(\tilde{x})$, as given in (24), and the boundedness of the state vector $\tilde{x}(t)$, permit the 7th-order plant system, as given by matrix A_{plant}, to be handled as an independent nonautonomous uniformly globally asymptotically stable (UGAS) system of the form

$$\dot{x} = A_{\text{plant}}(x(t), t)\,x \tag{29}$$

i.e., it is proven that for each pair of strictly positive real scalars (ρ, θ), there exists $T > 0$ such that for each solution

$$\|x_o\| \leq \rho \Rightarrow \|x(t, t_o, x_o)\| \leq \theta\ \forall t \geq t_o + T. \tag{30}$$

Adding to the system (29) the external input vector ϵ we arrive at

$$\dot{x} = A_{\text{plant}}(x(t), t)\,x + B_{\text{plant}}\epsilon. \tag{31}$$

For system (31), we will prove total stability. As it is pointed out in [27], if we consider a system of the form

$$\dot{x} = f(x, t) + u \tag{32}$$

and the solution of the unforced system ($u = 0$) is uniformly asymptotically or exponentially stable, then system (32) is totally stable, i.e., for each $\eta > 0$, there exist two positive scalars δ_1 and δ_2 such that

$$\|x_o\| \leq \delta_1, \quad \|u\| \leq \delta_2 \Rightarrow \|x(t, t_o, x_o, u)\| \leq \eta\ \forall t \geq t_o. \tag{33}$$

From (31), we can see that there exists suitable constant $B_{\text{plant}}\epsilon$ such that the system states remain bounded. In addition, it is pointed out that by selecting $r = 1$ in the control law, a unique constant equilibrium $\tilde{x}^*$ can be found in the bounded area for the permitted ϵ. ■

To prove that the solution $\tilde{x}(t)$ will converge to the equilibrium $\tilde{x}^*$, the analysis described by the authors in [11], [12] can be used to provide a suitable switching storage function that proves convergence. Particularly, closed-loop system (22) is indeed in Hamiltonian-passive form with Hamiltonian storage function given by (27). The equilibrium $\tilde{x}^*$ of (22), corresponding to $\omega_r^* = \omega_r^{\text{ref}}$ and $i_{ds}^* = i_{ds}^{\text{ref}}$ that satisfies $\dot{V}(\tilde{x}^*) = 0$ can be considered, under the assumptions discussed in the previous analysis, to lie in the range wherein $\tilde{x}$ is bounded. Therefore, Assumptions 1–3 posed in [11] are relaxed in the present case where a particular structure of a Hamiltonian-passive system is considered. In addition, this makes possible: 1) the significant modification of the proposed controller with respect to the one described as generalized stabilizing controller in [11] such that the new bounded requirements for the duty-ratio to be fulfilled and 2) a substantial simplification of the proof processing for Proposition 1; as it is already seen, this proof is based on classic nonlinear analysis [27]

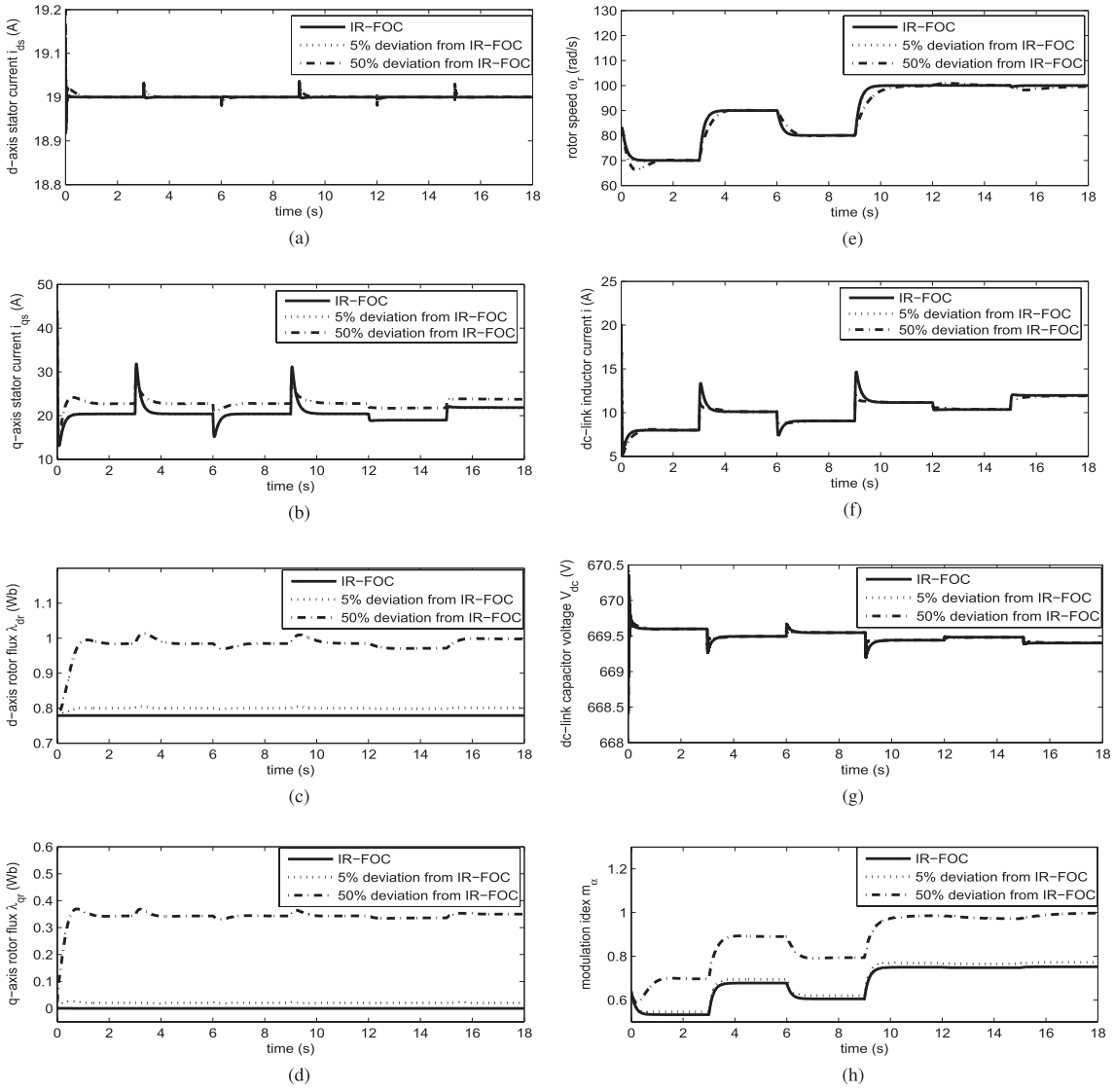

Fig. 4. Complete system response with the proposed controller. (a) d-axis stator current. (b) q-axis stator current. (c) d-axis rotor flux. (d) q-axis rotor flux. (e) motor speed. (f) dc-link inductor current. (g) dc-link capacitor voltage. (h) Modulation index.

and the process used is totally different from that presented in [11], where the theory of linear approximations is used [28]. Therefore, for system (22), Lemma 3 of [11] holds true as an immediate result of Proposition 1. This can be easily proven because boundedness of solution $\tilde{x}(t)$ implies upper and lower bounds for $V(\tilde{x}(t))$, i.e., $V_{\min} \leq V(\tilde{x}(t)) \leq V_{\max}$. Thus, it certainly holds true that a suitable switching storage function (differentiable nonincreasing), for the complete system (22), exists. For the reader's convenience, the analytic proof with the switching storage function construction is omitted here to avoid an unnecessary repetition. Thus, finally, LaSalle's Invariance Principle can be directly applied to prove convergence to the unique equilibrium resulting in the following Proposition.

Proposition 2: The solution $\tilde{x}(t)$ of the closed-loop system (22) satisfying the assumptions of Proposition 1, converges to the unique equilibrium $\tilde{x}^*$ as $t \to \infty$.

Hence, Proposition 2 guarantees that there are acceptable changes on ω_r^{ref} or on the external torque T_L that lead states z_1, z_2 to a new equilibrium on disk D of Fig. 2.

TABLE I
SYSTEM PARAMETERS

motor rated power P_n	$22.4kW$
rated stator voltage V_s	$230V$
rated stator current I_s	$39.5A$
rated speed ω_n	$1168rpm$
diode rectifier output V_{rec}	$670V$
dc-link capacitance C	$1.2mF$
dc-link inductance L	$1mH$
dc-link resistance R_L	$0,05Ohm$
stator inductance L_s	$44.2mH$
rotor inductance L_r	$41.7mH$
mutual inductance L_m	$41mH$
stator resistance R_s	$0.294Ohm$
rotor resistance R_r	$0.156Ohm$
pole pairs p	3
motor-load inertia J_m	$0.4kg \cdot m^2$
friction coefficient b	$0.003N \cdot m \cdot s/rad$

V. SIMULATION RESULTS

To test and verify the controller efficiency, the complete inverter-motor system is simulated for an industrial size

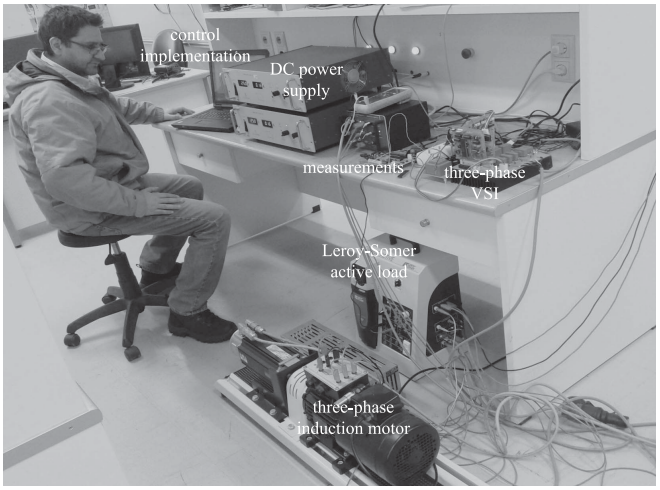

Fig. 5. Experimental setup.

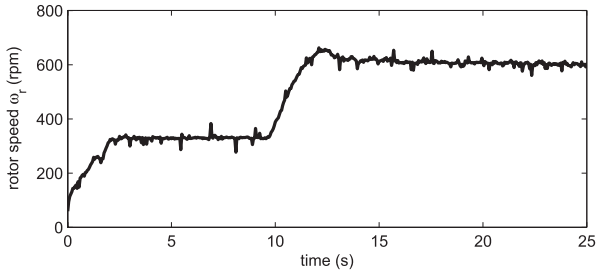

Fig. 6. Experimental results under speed reference changes.

22.4-kW induction motor. The system parameters are shown in Table I.

For the proposed nonlinear controller the gains are selected to be $k_1 = 0.05$ s/rad, $k_2 = -30$ A^{-1}, whereas constant $c = 1000$ and the initial conditions are $z_1(0) = 0.6370$, $z_2(0) = 0.0508$, and $z_3(0) = 0.7692$ satisfying the constraint $r = 1$.

Starting from an arbitrary initial point, the reference motor speed is set to $\omega_r^{\text{ref}} = 70$ rad/s and the reference d-axis current is set to $i_{ds}^{\text{ref}} = 19$ A. At time instant $t_1 = 3$ s, the desired motor speed rises to $\omega_r^{\text{ref}} = 90$ rad/s, at time instant $t_2 = 6$ s drops to $\omega_r^{\text{ref}} = 80$ rad/s, and at time instant $t_3 = 9$ s it changes to $\omega_r^{\text{ref}} = 100$ rad/s.

To check the controller performances under sudden load torque changes, at time instant $t_4 = 12$ s, while the motor speed is operating at steady-state on its constant reference value 100 rad/s, the load toque T_L drops from 70 to 65 N · m and at time instant $t_5 = 15$ s, it changes to 75 N · m. The same scenario is illustrated in the cases where the actual rotor time constant τ_r is increased by 5% and 50% without being considered in the controller (inaccurate rotor time constant).

Fig. 4 shows the time response of the system states and the modulation index m_a. In both cases of accurate and inaccurate rotor time constant, the proposed controller suitably regulates the d-axis stator current and the motor speed to their desired values, as shown in Figs. 4(a) and (e), respectively, independently from any rapid changes of the reference speed or the load torque. In Fig. 4(d), we can observe that, in the first case, field orientation is guaranteed at steady-state, as

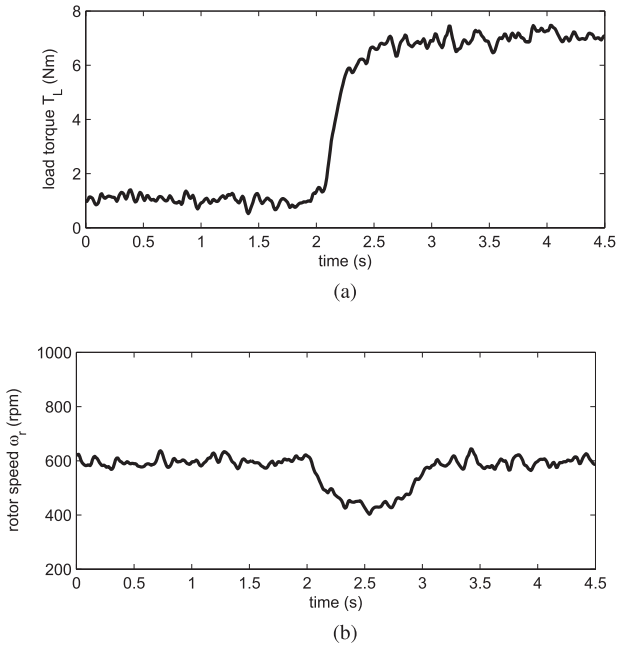

Fig. 7. Experimental results under torque changes. (a) Load torque. (b) Motor speed.

expected, because the q-axis rotor flux is regulated to the zero value, whereas in the case where a mismatch occurs on the time constant τ_r, the q-axis rotor flux is not zero. As shown in Fig. 4(g), the dc-link capacitor voltage response is almost the same in all the cases. The rest of the states, as shown in Figs. 4(b), (c), and (f) and the duty-ratio input shown in Fig. 4(h), are regulated to different steady-state values for each case, corresponding to the different equilibriums. The time response of the modulation index m_a of the inverter, as given by (11), is shown in Fig. 4(h), where it is clear that the proposed controller guarantees linear modulation. Hence, the proposed controller provides a closed-loop system with a very good performance, ensures speed regulation and indicates a stable operation with convergence to the desired equilibriums independently from the accurate field-oriented operation.

VI. Experimental Results

To further verify the proposed controller efficiency, experimental results are conducted for a lab size 1.5-kW three-phase induction motor. The experimental setup is shown in Fig. 5.

The experimental setup consists of a dc power supply, a three-phase VSI that operates according to the proposed control design, a three-phase induction motor from Leroy-Somer (LSVMV90LT), the Leroy-Somer active load that allows load torque changes and provides rotor speed and torque measurements and additional current transducers for the required stator current measurements. The proposed controller is implemented using a PC (notebook) and is transferred to the microprocessor on the board connected to the VSI. The inverter operates using sinusoidal PWM with switching frequency 10 kHz.

The induction motor parameters are: 1) $P_n = 1.5$ kW; 2) $V_n = 380$ V; 3) $\omega_n = 1425$ rpm; 4) $J = 0.0049$ kg · m^2; and 5) $p = 2$.

$$\tilde{J} = \begin{bmatrix} 0 & \sigma\omega_s & 0 & 0 & \frac{L_m}{L_r} p\lambda_{qr} & 0 & 2z_1 & 0_{1\times 3} \\ -\sigma\omega_s & 0 & 0 & 0 & -\frac{L_m}{L_r} p\lambda_{dr} & 0 & 2z_2 & 0_{1\times 3} \\ 0 & 0 & 0 & \frac{1}{\tau_r L_r i_{ds}^{\text{ref}}} & 0 & 0 & 0 & 0_{1\times 3} \\ 0 & 0 & -\frac{1}{\tau_r L_r i_{ds}^{\text{ref}}} & 0 & 0 & 0 & 0 & 0_{1\times 3} \\ -\frac{L_m}{L_r} p\lambda_{qr} & \frac{L_m}{L_r} p\lambda_{dr} & 0 & 0 & 0 & 0 & 0 & 0_{1\times 3} \\ 0 & 0 & 0 & 0 & 0 & 0 & -\frac{2}{3} & 0_{1\times 3} \\ -2z_1 & -2z_2 & 0 & 0 & 0 & \frac{2}{3} & 0 & 0_{1\times 3} \\ 0_{3\times 1} & 0_{3\times 1} & 0_{3\times 1} & 0_{3\times 1} & 0_{3\times 1} & 0_{3\times 1} & 0_{3\times 1} & J_c \end{bmatrix}$$

Two different scenarios are illustrated using the same proposed nonlinear controller. In all the cases, the desired d-axis stator current is set to 0.7 A according to the system parameters. The rotor time constant is not known exactly, thus investigating the case of inaccurate field orientation.

In the first case, starting from a very low speed of about 100 rpm, the desired motor speed ω_r^{ref} is gradually set at 330 rpm, whereas at time instant $t = 10$ s the reference speed changes to 600 rpm. From Fig. 6, the proposed controller suitably tracks the motor speed at the desired levels verifying a satisfactory performance even in low and very low speeds.

In the second scenario, while the motor speed is regulated at $\omega_r^{\text{ref}} = 600$ rpm, a large step change is applied at the load torque T_L from 1 to $7N \cdot m$ at time instant $t = 2$ s. The load torque change is shown in Fig. 7(a), whereas the time response of the motor speed is shown in Fig. 7(b). We can easily see that the motor speed is quickly regulated at its reference value after this large variation of the load, confirming the good response of the proposed control scheme.

VII. Conclusion

In this brief, the development of a new nonlinear controller for VSI-fed induction motors with some advanced characteristics was given. A detailed stability analysis was conducted that considered the dynamics of the entire VSI/motor system. Stability and convergence to the equilibrium were theoretically proven and verified by extensive tests. Particularly, in accurate as well as inaccurate field-oriented operation, a very satisfactory system response was observed. The controller task, that was the rotor speed regulation, was successfully achieved in both the cases and under large reference speed and load torque changes.

Appendix

See equation at the top of the page, where ω_s is given by (21) and

$$J_c = \begin{bmatrix} 0 & 0 & -k_1\left(i_{ds} - i_{ds}^{\text{ref}}\right) \\ 0 & 0 & -k_2\left(\omega_r - \omega_r^{\text{ref}}\right) \\ k_1\left(i_{ds} - i_{ds}^{\text{ref}}\right) & k_2\left(\omega_r - \omega_r^{\text{ref}}\right) & 0 \end{bmatrix}.$$

Acknowledgment

The authors would like to thank Associate Editor Prof. F. Vasca for his valuable suggestions and guidelines and the anonymous reviewers for their comments and remarks that made possible the enhancement of this brief.

References

[1] B. K. Bose, *Modern Power Electronics and AC drives*. Upper Saddle River, NJ, USA: Prentice-Hall, 2002.
[2] N. P. Quang and J.-A. Dittrich, *Vector Control of Three-Phase AC Machines: System Development in the Practice*. New York, NY, USA: Springer-Verlag, 2008.
[3] J. Chiasson, "A new approach to dynamic feedback linearization control of an induction motor," *IEEE Trans. Autom. Control*, vol. 43, no. 3, pp. 391–397, Mar. 1998.
[4] Y. Wang, Z. Wang, J. Yang, and R. Pei, "Speed regulation of induction motor using sliding mode control scheme," in *Proc. 40th IAS Annu. Meeting*, Oct. 2005, pp. 72–76.
[5] R. Ortega, A. Loria, P. J. Nicklasson, and H. Sira-Ramirez, *Passivity-Based Control of Euler-Lagrange Systems*. New York, NY, USA: Springer-Verlag, 1998.
[6] Z. Xu, J. Wang, and P. Wang, "Passivity-based control of induction motor based on euler-lagrange (EL) model with flexible damping," in *Proc. Int. Conf. Electr. Mach. Syst. ICEMS*, 2008, pp. 48–52.
[7] T.-S. Lee, "Lagrangian modeling and passivity-based control of three-phase AC/DC voltage-source converters," *IEEE Trans. Ind. Electron.*, vol. 51, no. 4, pp. 892–902, Aug. 2004.
[8] J.-J. Wang and J. He, "Torque and flux direct backstepping control of induction motor," in *Proc. 7th WCICA*, Jun. 2008, pp. 6407–6410.
[9] R. Trabelsi, A. Khedher, M. F. Mimouni, and F. M'Sahli, "An adaptive backstepping observer for on-line rotor resistance adaptation," *Int. J. Sci. Tech. Autom. Control Comput. Eng.*, vol. 4, no. 1, pp. 1246–1267, 2010.
[10] D. Novotny and T. Lipo, *Vector Control of AC Drives*. Oxford, U.K.: Clarendon Press, 1996.
[11] G. C. Konstantopoulos and A. T. Alexandridis, "Generalized nonlinear stabilizing controllers for Hamiltonian-passive systems with switching devices," *IEEE Trans. Control Syst. Technol.*, vol. 21, no. 4, pp. 1479–1488, Jul. 2013.
[12] G. C. Konstantopoulos and A. T. Alexandridis, "Stability and convergence analysis for a class of nonlinear passive systems," in *Proc. 50th IEEE Conf. Decision Control Eur. Control Conf.*, Dec. 2011, pp. 1753–1758.
[13] M. N. Marwali, A. Keyhani, and W. Tjanaka, "Implementation of indirect vector control on an integrated digital signal processor-based system," *IEEE Trans. Energy Convers.*, vol. 14, no. 2, pp. 139–146, Jun. 1999.
[14] P. A. De Wit, R. Ortega, and I. Mareels, "Indirect field-oriented control of induction motors is robustly globally stable," *Automatica*, vol. 32, no. 10, pp. 1393–1402, 1996.
[15] W.-J. Wang and J.-Y. Chen, "Compositive adaptive position control of induction motors based on passivity theory," *IEEE Trans. Energy Convers.*, vol. 16, no. 2, pp. 180–185, Jun. 2001.
[16] G. Chang, J. P. Hespanha, A. S. Morse, M. Netto, and R. Ortega, "Supervisory field-oriented control of induction motors with uncertain rotor resistance," *Int. J. Adapt. Control Signal Process.*, vol. 15, no. 3, pp. 353–375, 2001.
[17] R. Reginatto and A. S. Bazanella, "Robustness of global asymptotic stability in indirect field-oriented control of induction motors," *IEEE Trans. Autom. Control*, vol. 48, no. 7, pp. 1218–1222, Jul. 2003.

[18] H. A. Toliyat, E. Levi, and M. Raina, "A review of RFO induction motor parameter estimation techniques," *IEEE Trans. Energy Convers.*, vol. 18, no. 2, pp. 271–283, Jun. 2003.

[19] R. Ortega, P. J. Nicklasson, and G. Espinosa-Perez, "On speed control of induction motors," *Automatica*, vol. 32, no. 3, pp. 455–460, 1996.

[20] S. Peresada, A. Tonielli, and R. Morici, "High-performance indirect field-oriented output-feedback control of induction motors," *Automatica*, vol. 35, no. 6, pp. 1033–1047, 1999.

[21] D. Karagiannis, A. Astolfi, R. Ortega, and M. Hilairet, "A nonlinear tracking controller for voltage-fed induction motors with uncertain load torque," *IEEE Trans. Control Syst. Technol.*, vol. 17, no. 3, pp. 608–619, May 2009.

[22] P. J. Nicklasson, R. Ortega, G. Espinosa-Perez, and C. Jacobi, "Passivity-based control of a class of blondel-park transformable electric machines," *IEEE Trans. Autom. Control*, vol. 42, no. 5, pp. 629–647, May 1997.

[23] S. Peresada and A. Tonielli, "High-performance robust speed-flux tracking controller for induction motor," *Int. J. Adapt. Control Signal Process.*, vol. 14, nos. 2–3, pp. 177–200, 2000.

[24] A. Behal, M. Feemster, and D. Dawson, "An improved indirect fiel-doriented controller for the induction motor," *IEEE Trans. Control Syst. Technol.*, vol. 11, no. 2, pp. 248–252, Mar. 2003.

[25] N. Mohan, T. M. Underland, and W. P. Robbins, *Power Electronics*. New York, NY, USA: Wiley, 2003.

[26] A. van der Schaft, *L_2-Gain and Passivity in Nonlinear Control*. New York, NY, USA: Springer-Verlag, 1999.

[27] J.-J. E. Slotine and W. Li, *Applied Nonlinear Control*. Upper Saddle River, NJ, USA: Prentice-Hall, 1991.

[28] M. Tomas-Rodriguez and S. P. Banks, *Linear, Time-Varying Approx-imations to Nonlinear Dynamical Systems: With Applications in Control and Optimization*. New York, NY, USA: Springer-Verlag, 2010.